Improving curcumin solubility and bioavailability by encapsulation in saponin-coated curcumin nanoparticles prepared using a simple pH-driven loading method

Journal:	*Food & Function*
Manuscript ID	FO-ART-11-2017-001814.R1
Article Type:	Paper
Date Submitted by the Author:	15-Feb-2018
Complete List of Authors:	McClements, David; University of Massachusetts, Food Science Peng, Shengfeng; Nanchang University - Qingshanhu Campus North, State Key Laboratory of Food Science and Technology Li, Ziling; State Key Laboratory of Food Science and Technology, Nanchang University, Nanchang 330047, Jiangxi, PR China Zou, Liqiang; Nanchang University, State Key Laboratory of Food Science and Technology Liu, Wei; Nanchang University, State Key Laboratory of Food Science and Technology Liu, Chengmei; nanchang university, State Key Laboratory of Food Science and Technology

Improving curcumin solubility and bioavailability by encapsulation in saponin-coated curcumin nanoparticles prepared using a simple pH-driven loading method

Shengfeng Peng [a], Ziling Li [ab], Liqiang Zou [a], Wei Liu *[a], Chengmei Liu [a], David Julian McClements *[c].

[a] State Key Laboratory of Food Science and Technology, Nanchang University, Nanchang 330047, Jiangxi, PR China

[b] School of Life Science, Jiangxi Science and Technology Normal University, Nanchang, 330013, Jiangxi, PR China

[c] Biopolymers and Colloids Laboratory, Department of Food Science, University of Massachusetts, Amherst, MA 01003, USA

Journal: Food and Function

Submitted: November 2017

Corresponding author:

E-mail: liuwei@ncu.edu.cn; Fax: +86 791 88334509; Tel: + 86 791 88305872x8106.

E-mail: mcclements@foodsci.umass.edu; Fax: +1 413 545 1262; Tel: +1 413 545 1019.

Abstract

Curcumin is a bioactive phytochemical that can be utilized as a nutraceutical or pharmaceutical in functional foods, supplements, and medicines. However, the application of curcumin as a nutraceutical in commercial food and beverage products is currently limited by its low water-solubility, chemical instability, and poor oral bioavailability. In this study, all-natural colloidal delivery systems were developed to overcome these challenges, which consisted of saponin-coated curcumin nanoparticles formed using a pH-driven loading method. The physicochemical and structural properties of the curcumin nanoparticles formed using this process were characterized, including particle size distribution, surface potential, morphology, encapsulation efficiency, and loading capacity. Fourier transform infrared spectroscopy and X-ray diffraction indicated that curcumin was present in the nanoparticles in an amorphous form. The curcumin nanoparticles were unstable to aggregation at low pH values (< 3) and high NaCl concentrations (> 200 mM), which was attributed to a reduction in electrostatic repulsion between them. However, they were stable at higher pH values (3 to 8) and lower NaCl levels (0 to 200 mM), due to a stronger electrostatic repulsion between them. They also exhibited good stability during refrigerated storage (4 °C) or after conversion into a powdered form (lyophilized). A simulated gastrointestinal tract study demonstrated that the *in vitro* bioaccessibility was around 3.3-fold higher for curcumin nanoparticles than for free curcumin. Furthermore, oral administration to Sprague Dawley rats indicated that the *in vivo* bioavailability was around 8.9-fold higher for curcumin nanoparticles than for free curcumin. These results have important implications for the development of curcumin-enriched functional foods, supplements, and drugs.

Keywords: curcumin; pH-driven; saponin; biosurfactant; nanoparticles, bioavailability.

1. Introduction

Curcumin is a hydrophobic polyphenol derived from turmeric (*Curcuma longa*) that exhibits a range of potentially beneficial biological and pharmacological effects, including antioxidant, antimicrobial, anti-inflammatory, and anticancer activities [1]. However, it is difficult to formulate curcumin-enriched functional foods and beverages due to its poor water-solubility, chemical instability (particularly under neutral and basic conditions), and low and variable oral bioavailability [2]. Consequently, researchers are developing various kinds of colloidal delivery systems to overcome these challenges, including micelles, microemulsions, nanoemulsions, emulsions, solid lipid nanoparticles, and microgels [3-6]. Micellar systems are particularly attractive for this purpose because they are thermodynamically stable, optically transparent, water-dispersible, and may be designed to enhance bioavailability [7]. Traditionally, micellar systems are assembled from small molecule synthetic surfactants, which consist of a polar head-group and a non-polar tail-group [8]. The surfactants spontaneously self-assemble in water due to the hydrophobic effect, which leads to the formation of micelles where the non-polar tails form a hydrophobic environment within the interior, and the polar heads form a hydrophilic shell at the exterior. Hydrophobic nutraceuticals, such as curcumin, can then be loaded into the interior of the micelles to form a water-dispersible colloidal delivery system [9]. There is currently great interest in the food industry in replacing synthetic surfactants with natural alternatives due to increasing consumer demand for "clean label" products [10]. Hence, it would be beneficial to be able to load curcumin into micelles formed from natural surfactants.

In the current study, we examined the possibility of incorporating curcumin into surfactant micelles assembled from saponins [11]. Saponins are secondary metabolites produced at appreciable levels by many types of plant species because of their ability to act as chemical defense systems against pathogens and herbivores [12]. Early research led to saponins being classified as anti-nutritional

factors because of their ability to disrupt cell membranes, such as those in red blood cells and fungi [13]. However, more recent research has led some researchers to question this classification [14]. For instance, consumption of certain types of saponins has been reported to decrease blood cholesterol levels, reduce cancer risk, and inhibit cancer cell growth [15]. Saponins have also been widely evaluated for their ability to form and stabilize oil-in-water emulsions and nanoemulsions [16, 17]. However, there have been few studies on their use to form curcumin-loaded lipid nanoparticles based on a surfactant micelle loading mechanism.

The main objective of the current study was therefore to investigate the potential of saponins for encapsulating curcumin and increasing its oral bioavailability. Curcumin was solubilized within the saponin micelles using a pH-driven loading method, and then the impact of environmental conditions on the properties and stability of the curcumin nanoparticles formed was measured. The potential gastrointestinal fate of the curcumin nanoparticles was then established using both *in vitro* (simulated gastrointestinal tract) and *in vivo* (oral administration to rats) studies. The results of this research may lead to novel food-grade colloidal delivery systems suitable for incorporating curcumin into food, supplement, or pharmaceutical products.

2 Materials and methods

2.1 Materials

Curcumin (98%) and saponin (sapogenin 20-35 %) were purchased from Aladdin Industrial Corporation (Shanghai China). Ethanol, phosphoric acid, sodium hydroxide and all other reagents used were of analytical grade and purchased from Xilong Chemical Co., (Shanghai, China).

2.2 Preparation of curcumin nanoparticles

Curcumin nanoparticles were prepared using a pH-driven method as described in our previous study with some slight modifications [18]. A schematic representation of this process is shown in **Fig. 1**. Briefly, an acidic aqueous surfactant solution was prepared by dissolving saponin in 20 mM phosphoric acid

at concentrations of 2, 4, 8, 12 and 16 mg/mL (pH 3). A basic aqueous curcumin solution (2.0 mg/mL) was prepared by dissolving curcumin in 30 mM sodium hydroxide solution (pH 12). Curcumin solutions were then added to saponin solutions (1:1 v/v) while being continuously stirred at 500 rpm on a magnetic stir-plate. The resulting solution was incubated for 0.5 h at room temperature and then centrifuged at 10,000 g for 10 min to remove any free curcumin and larger particulate matter. It is proposed that this process leads to the formation of saponin-coated curcumin nanoparticles due to movement of curcumin molecules into the hydrophobic cores of saponin micelles (**Fig. 1**). As shown in **Fig. 1C**, after the basic curcumin was added into the acid saponin solutions, the pH rapidly increased to around pH 6.5 within 10 second. Thus, the whole process was very fast and the system reached equilibrium in a short time.

2.3 Characterizations of curcumin nanoparticles

The particle size distribution, mean particle diameter, and surface potential (ζ-potential) of the curcumin nanoparticles were measured at 25°C using a combined dynamic laser light scattering (DLS) – electrophoresis instrument (Nicomp 380 ZLS, Santa Barbara, CA, USA). The particle size was determined by measuring the intensity fluctuations of the light scattered at an angle of 90° from the sample, and then fitting an appropriate mathematical model to the data using the instrument software. The ζ-potential of the particles was determined by measuring the velocity and direction that they moved in a well-defined electrical field. The samples were diluted 4-fold in water before analysis to avoid multiple scattering effects. All the data is reported as the mean and standard deviation based on measurements carried out on at least three samples with each sample being analyzed in triplicate.

Microstructure images of the samples were obtained using Atomic Force Microscopy (AFM, Agilent 5500, Agilent Technologies, Santa Clara, CA, USA). A small aliquot of a suspension of curcumin nanoparticles was placed on a freshly cleaved mica substrate, and then images of the sample were acquired

using the AFM operated at room temperature with a silicon cantilever force constant of 0.58 N m^{-1} in tapping mode.

X-ray diffraction (XRD) patterns of powdered crystalline curcumin and curcumin nanoparticles were recorded using an X-ray diffractometer (D8 Advance, Bruker, Germany). The divergence slit was set at 1°, and the receiving slit was set at 0.1 mm for the incident beam. The scan rate was 2° per min over a 2θ angle range of 5° – 40°.

Infrared spectra of curcumin, saponin, and curcumin nanoparticles were obtained using a Fourier transform infrared (FTIR) spectrophotometer (Nicolet 5700, Thermo Electron Co., Waltham, MA, USA). Transmission spectra were recorded over the wave number range of 4000-400 cm^{-1}.

The encapsulation efficiency (EE) and loading capacity (LC) of the nanoparticles were determined using the methods described in our previous study [18]. Briefly, a suspension of curcumin nanoparticles was centrifuged at 10,000 g for 10 min to remove any non-encapsulated curcumin. The supernatant was then removed and diluted with anhydrous ethanol. The absorbance of the samples at 420 nm was then measured using a UV-Vis spectrophotometer (Pgeneral T6, China) and the concentration of loaded curcumin was determined from a calibration curve. The encapsulation efficiency and loading capacity of the nanoparticles were then calculated using the following expressions:

$$EE\ (\%) = m_{C,L} / m_{C,I} \times 100 \quad (1)$$

$$LC\ (\%) = m_{C,L} / m_{M} \times 100 \quad (2)$$

Here, $m_{C,L}$ is the mass of curcumin loaded into the saponin-coated curcumin nanoparticles, $m_{C,I}$ is the initial mass of curcumin in the system, and m_M is the mass of the saponin-coated curcumin nanoparticles (curcumin + saponin). The value of m_M was determined by freeze drying the suspension of centrifuged curcumin nanoparticles to remove any water. The concentration of curcumin

remaining after lyophilization and rehydration was determined as described above.

2.4 Physical stability of curcumin nanoparticles

Influence of pH: Aqueous dispersions of curcumin nanoparticles were adjusted to pH values ranging from 2.0 to 8.0 using either HCl or NaOH solutions.

Influence of ionic strength: Different amounts of sodium chloride were added to aqueous dispersions of curcumin nanoparticles and then stirred for 1 hour at ambient temperature to obtain a series of samples with different salt levels: of 10, 20, 50, 100, 200 and 1000 mM NaCl.

Storage stability: The stability of curcumin nanoparticles was measured during storage in powdered form (lyophilized) at 25 ºC or during storage in aqueous solutions at 4 or 25 ºC.

The stability of the curcumin nanoparticles was assessed by measuring changes in their appearance, particle size, and ζ-potential after exposure to the above conditions.

2.5 In vitro bioavailability

2.5.1. Simulated gastrointestinal tract

The potential gastrointestinal fate of the curcumin nanoparticles was established by passing them through a simulated gastrointestinal tract (GIT) consisting of mouth, stomach, and small intestine phases, as described in our previous study [18].

Mouth phase: 7.5 mL of curcumin nanoparticle suspension were mixed with 7.5 mL of simulated saliva fluid containing mucin (30 mg/mL), together with various salts, as described elsewhere [19]. The resulting mixtures were then adjusted to pH 6.8 and shaken at 90 rpm for 10 min at 37 °C to mimic oral conditions.

Stomach phase: Simulated gastric fluid was prepared by adding NaCl (2 mg/mL), HCl (7 mg/mL), and pepsin (3.2 mg/mL) to distilled water and then warming to 37 °C. 15 mL of this simulated gastric fluid was then added to the 15

198 mL of sample resulting from the mouth phase. The mixture was then adjusted to
199 pH 2.5 and shaken at 100 rpm for 2 h to mimic stomach conditions.
200 *Small intestine phase*: Samples from the simulated gastric phase were adjusted
201 to pH 7.0 using 2 M NaOH solution. Simulated small intestinal fluids containing
202 pancreatin (24 mg/mL, 2.5 mL), bile extract solution (50 mg/mL, 3.5 mL) and
203 saline solution (0.5 M $CaCl_2$ and 7.5 M NaCl, 1.5 mL) were then added. The pH
204 of the resulting mixture was then maintained constant at pH 7.0 by addition of 50
205 mM NaOH using an automatic titration device (pH-stat).
206 *2.5.2. Curcumin stability and bioaccessibility*
207 The *in vitro* bioavailability of the curcumin was assumed to be primarily
208 determined by its chemical transformation and bioaccessibility within the GIT
209 model [20]. After passage through the simulated mouth, stomach, and small
210 intestine phases, the raw digesta were collected and centrifuged at 40,000 g for 30
211 min at 4°C. The resulting supernatants were collected and assumed to be the
212 dietary mixed micelle fraction, in which the curcumin was solubilized in a
213 bioaccessible form. The solubilized curcumin was diluted with methanol and
214 assayed using a 1260 HPLC system (Agilent Technologies, Santa Clara, CA,
215 USA) equipped with a UV-vis detector. Curcumin was separated on a Sunfire C
216 18 column (250 mm × 4.6 mm, 5 μm; Waters Corporation, Milford, MA, USA),
217 using a mobile phase consisting of 0.1% (v/v) acetic acid and acetonitrile (45:55
218 v/v) at a flow rate of 1.0 mL min^{-1}, with detection by UV absorption at 420 nm.
219 The stability and bioaccessibility of the curcumin were calculated using the
220 following equations:
221 $$\text{Stability (\%)} = C_{Digesta} / C_{Initial} \times 100 \quad (3)$$
222 $$\text{Bioaccessibility (\%)} = C_{Micelles}/C_{Digesta} \times 100 \quad (4)$$
223 Here, $C_{Initial}$ is the initial concentration of curcumin in the system (taking into
224 account the various dilution steps), while $C_{Micelles}$ and $C_{Digesta}$ are the curcumin
225 concentrations in the mixed micelle fraction and in the overall digesta after
226 exposure to the simulated GIT, respectively. The $C_{Initial}$ value is equal to the

amount of curcumin that would be present in the small intestine phase if there were no losses due to chemical degradation during passage of the sample through the simulated GIT.

2.6 In vivo bioavailability

The *in vivo* bioavailability of free curcumin and curcumin nanoparticles was evaluated using 12 male Sprague Dawley (SD) rats that weighed between 260 and 300 g. All experimental procedures were performed in accordance with the Guidelines for Care and Use of Laboratory Animals and approved by the Animal Ethics Committee of Nanchang University, and animal handling followed the dictates of the National Animal Welfare Law of China. The rats were randomly divided into two groups (n=6). Group 1 was administrated 100 mg/kg body weight of free curcumin suspensions and Group 2 was administrated 100 mg/kg body weight of curcumin nanoparticles by oral gavage. Free curcumin suspensions (10 mg/mL) were prepared by dispersing powdered curcumin crystals in 1.0% sodium carboxymethyl cellulose, while curcumin nanoparticle suspensions (10 mg/mL) were prepared by dispersing lyophilized curcumin nanoparticles into distilled water. A total of 0.5 mL of blood samples were collected from the retro-orbital plexus of the rats at different times (0.5, 1, 2, 4 and 8 h) into heparinized microcentrifuge tubes (containing 20 μL of 1000 IU heparin/mL of blood). The samples were immediately centrifuged at 4000 g for 10 min at 4 °C to isolate the plasma, which was then stored at -80 °C until analysis by LC–MS/MS. According to previous studies [21-23], curcumin is mainly conjugated as curcumin glucuronide when it is absorbed through the intestinal cells of rats. So, the concentration of curcumin and curcumin glucuronide in the rat plasma were determined.

Plasma (100 μL) was mixed with 200 μL acetonitrile by vortexing and centrifuged at 10,000 g for 5 min at 4 °C. Aliquots of the extracts were injected onto a C18 column (Zorbax Eclipse Plus C18 column, 100mm×2.1mm, I.D., 3.5 μm, Agilent, USA) kept at 40 °C. The mobile phase consisted of two

components: A, acetonitrile and B, 0.1% formic acid. The gradient profile used during the analysis was as follows: 0-1 min, 80%B→20%B; 1-3 min, 20%; 3-3.5 min, 20%B→80%B. A flow rate of 0.3 ml/min was used. Curcumin and curcumin glucuronide were analyzed using a 6410 QQQ MS/MS system (Agilent Technologies, USA) equipped with an electrospray ionization source (ESI), operating in positive mode. The mass spectrometer ion source parameters were as follows: gas temperature, 350℃; gas flow rate, 10 L/min; nebulizer gas pressure, 40 psi; spray voltage, 4000 kV. Nitrogen gas served as the nebulizer and collision gas. Curcumin and curcumin glucuronide were determined using the multiple reaction monitor mode as follows: curcumin, m/z 369 > 285, m/z 369 >177. curcumin glucuronide, m/z 545 > 369, m/z 545 >177.

2.7. Statistical analysis

All measurements were replicated at least three times. The results are expressed as means ± standard deviations. Data were subjected to statistical analysis using SPSS software, version 18.0 (SPSS Inc., Chicago, IL, USA). The Student-Newman-Keuls test was performed to check significant comparisons and $P<0.05$ was considered statistically significant.

3 Results and discussion

3.1 Optimization and characterization of curcumin nanoparticles

Initially, experiments were carried out to characterize the properties of the saponin-coated curcumin nanoparticles prepared using the pH-driven loading method. The impact of saponin concentration on the physicochemical and structural properties of the curcumin nanoparticles is summarized in **Table 1**. Experiments were carried out with fresh nanoparticle suspensions, and with nanoparticle suspensions that had been converted into a powder using freeze-drying, and then rehydrated.

It should be noted that curcumin is known to chemically degrade when stored at alkaline conditions [2], and therefore there is some concern that it may be lost

during the pH-driven loading step. However, previous studies have shown that less than 6% of curcumin was lost after incubation in aqueous solutions at pH 12.0 for one hour [18, 24]. In the present study, the curcumin was only incubated at pH 12.0 for 5 min, and so the loss of curcumin from this process should be small.

3.1.1. Impact of saponin concentration

Initially, the impact of surfactant concentration on the formation of the curcumin nanoparticles was investigated. The mean particle diameter decreased from around 109 to 52 nm as the saponin level increased from 1 to 4 mg/mL, but then remained relatively constant (around 51 nm) when the saponin level was increased from 4 to 8 mg/mL. The polydispersity index of the nanoparticle suspensions was somewhat higher at low saponin levels (PDI =0.19-0.28 at 1 to 4 mg/mL) than at higher levels (PDI = 0.16-0.17 = at 6 to 8 mg/mL). The encapsulation efficiency of the curcumin nanoparticles increased from around 71 to 92% when the saponin concentration increased from 1 to 4 mg/mL, but then remained relatively constant when it was increased further. Taken together these results suggest that a certain amount of saponin is required to form small particles with a narrow size distribution and high encapsulation efficiency. The critical micelle concentration (CMC) of quillaja saponin has been reported to be around 0.5 to 0.8 mg/mL [25]. Consequently, at the lowest saponin levels used only a small fraction of the surfactant molecules actually self-assembled into micelles that could solubilize the curcumin. In addition, above the CMC, the solubilization capacity of the surfactant micelles would be expected to decrease with decreasing quillaja saponin concentration because there are less hydrophobic domains present to incorporate the curcumin. Thus, all of the curcumin could not be solubilized inside the surfactant micelles at relatively low saponin levels, leading to the presence of some free curcumin that formed relatively large crystals in the aqueous phase.

The curcumin-loaded nanoparticles were all negatively charged, however the magnitude of the ζ-potential depended on saponin concentration (Table 1). The

magnitude of the ζ-potential remained relatively high and constant (around -30 mV) when the saponin concentration increased from 1 to 4 mg/mL, but then decreased when it was further increased to 8 mg/mL (around -19 mV). A number of possible physicochemical phenomenon may account for this observation. First, commercial saponin ingredients have been reported to contain some residual mineral ions[26], and so there may have been some electrostatic screening of the surface potential of the colloidal particles at higher saponin levels due to accumulation of oppositely charged counter-ions around them[8]. Second, there may have been an increase in the viscosity of the aqueous phase surrounding the colloidal particles at higher surfactant levels, which would cause the measured ζ-potential to decrease [8]. Third, the composition of the colloidal particles (curcumin-to-saponin ratio) changed as the saponin concentration was increased, which may have altered their electrical characteristics. Fourth, there may have been some free curcumin crystals dispersed in the aqueous phase that contributed to the ζ-potential signal at low saponin levels, but these were solubilized at higher levels. Further research is clearly required to establish the physicochemical origin of this effect.

In general, a higher absolute value of the ζ-potential on colloidal particles leads to an increase in the electrostatic repulsion between them, which should increase their aggregation stability [8]. However, this was not the case for the colloidal dispersions prepared in this study, since the particles with the highest absolute value of the ζ-potential (low saponin levels), had the largest particle size (**Table 1**). This suggests that other factors were more important, such as the incorporation of all of the curcumin into the interior of the colloidal particles, and steric repulsion by the surfactant head groups.

3.1.2. Impact of freeze drying

In many commercial applications, it is more convenient to deliver curcumin in a powdered form, rather than in a liquid form. For this reason, the impact of freeze-drying and rehydration on the properties of the curcumin nanoparticles

342 was determined (**Table 1**).

343 As with the freshly prepared systems, the particle size and polydispersity of
344 the colloidal particles decreased with increasing saponin concentration, but the
345 values of the mean particle diameter and polydispersity index at low saponin
346 levels (1 to 4 mg/mL) were appreciably higher than those for the equivalent fresh
347 systems. On the other hand, the mean particle diameter and polydispersity index
348 were fairly similar at higher saponin levels for the two systems. These results
349 suggest that some particle aggregation occurred during the freeze-drying and/or
350 rehydration process when there was insufficient saponin present. Again, this may
351 have been due to the presence of some curcumin that had not been incorporated
352 into the hydrophobic interior of the colloidal particles, thereby leading to the
353 presence of curcumin crystals in the system. Presumably, these large curcumin
354 crystals are more susceptible to aggregation during dehydration/rehydration than
355 the small curcumin nanoparticles. These results show that curcumin-loaded
356 nanoparticles can be successfully converted into a powdered form that can be re-
357 dispersed in an aqueous solution, provided there is sufficient surfactant present.

358 For commercial applications, it is usually important to limit the total amount
359 of surfactant used in a product due to cost, taste, and toxicity concerns. For this
360 reason, a saponin level of 4 mg/mL was used in the remainder of the studies
361 because it was the lowest amount that led to relatively small curcumin
362 nanoparticles with a narrow particle size distribution and high encapsulation
363 efficiency.

364 **3.2 Characterization of curcumin nanoparticles**

365 In this section, a range of analytical methods was used to provide some insight
366 into the characteristics of the curcumin nanoparticles formed using the pH-driven
367 loading method.

368 *3.2.1. Particle size, morphology, and charge*

369 As discussed earlier, the dynamic light scattering measurements indicated that
370 the nanoparticles formed were relatively small (d = 52 nm) and had a narrow size

distribution (PDI = 0.242). Interestingly, the mean diameter of the curcumin-loaded colloidal particles was appreciably larger than the reported mean diameter (around 7 nm) of pure saponin micelles in aqueous solution [26]. This suggests that the saponin micelles must have incorporated an appreciable quantity of curcumin molecules into their hydrophobic interiors during the pH-driven loading process and thereby becoming highly swollen (**Fig. 1**). A relatively large mean particle diameter (130 nm) has also been reported for saponin micelles loaded with lutein esters using a direct mixing process [9]. As discussed earlier, the curcumin-loaded nanoparticles had a relatively high negative surface potential (ζ = -30.4 mV), which can be attributed to carboxyl groups on the sugar residues [11].

Atomic force microscopy was used to provide additional information about the size and morphology of the particles in the nanoparticle suspensions. The AFM images indicated that the saponin-coated curcumin nanoparticles were spherical and evenly distributed throughout the system, with dimensions consistent with those determined by dynamic light scattering (**Fig. 2**).

3.2.2. Encapsulation properties

The amount of a bioactive component that can be successfully loaded into a colloidal delivery system is important for commercial applications. The encapsulation efficiency and loading capacity of curcumin in the nanoparticles prepared in this study using the pH-driven loading method were 91.8 ± 2.8% and 15.3 ± 0.4%, respectively. These values compare well with several previous studies. An EE of 46% and LC of 4.4% were reported for curcumin solubilized in non-ionic surfactant micelles (1% Pluronic P123) in aqueous solutions using a heating method [27]. An EE of 89.3% and LC of 20.7% were reported for curcumin loaded into copolymer mPEG-PCL micelles using a nanoprecipitation method [28]. An EE of 81% and LC of 4% were reported for curcumin loaded into casein micelles by a pH-driven method [24]. Consequently, the saponins used in our study appear to be as effective as other types of synthetic and natural surfactants at encapsulating curcumin.

3.2.3. Molecular interactions and physical state

Information about the molecular interactions and physical state of the curcumin in the saponin-coated nanoparticles was obtained using Fourier transform infrared and X-ray diffraction. The FTIR spectra of pure curcumin (a), pure saponin (b) and saponin-coated curcumin nanoparticles (c) are shown in **Fig. 3.** A number of peaks were observed in the pure curcumin spectrum, which were assigned to different functional groups based on previous research: 3508 cm^{-1} (–OH stretching vibration on benzene ring); 1628 cm^{-1} (C=C and C=O vibration); 1601 cm^{-1} (stretching vibrations of benzene ring); 1508 cm^{-1} (C=O and C=C vibrations); 1427 cm^{-1} (olefinic C–H bending vibrations); 1276 cm^{-1} (aromatic C–O stretching vibrations); 1026 cm^{-1} (C–O–C stretching vibrations) and 961 cm^{-1} (benzoate trans-CH vibrations) [29]. Numerous peaks were also observed in the pure saponin spectrum: 3419 cm^{-1} (O-H stretching vibrations); 2936 cm^{-1} (the antisymmetric stretching vibration of saturated $–CH_2$); 1719 cm^{-1} (ketones group C=O stretching vibrations); 1617 cm^{-1} (C=C stretching vibrations); 1380 cm^{-1} (symmetrical formation vibration of $–CH_3$); and 878 to 1159 cm^{-1} (C–O–C absorption) [30, 31]. As expected, when curcumin was loaded into the saponin micelles, some of the peaks corresponded to those observed in the pure saponin spectrum, while others corresponded to those observed in the pure curcumin spectrum. For instance, the FTIR spectrum for the saponin-coated curcumin nanoparticles exhibited peaks at 1628 cm^{-1}, 1516 cm^{-1} and 1282 cm^{-1}, which confirmed that the nanoparticles actually contained curcumin. However, the peaks corresponding to curcumin in the saponin-coated curcumin nanoparticles were shifted when compared to those of pure curcumin (from 1508 to 1516 cm^{-1}), which suggested an interaction between curcumin and saponin. The curcumin peak at 1276 cm^{-1} shifted to 1282 cm^{-1}, which may be due to a change in the stretching and bending vibrations of different C-O groups [32]. According to our previous study [33], the disappearance of the 3508 cm^{-1} peak in the spectrum obtained for the curcumin nanoparticles is indicative of an interaction of the phenolic –OH of curcumin with saponin, most likely through hydrogen bonding.

A number of the major absorption peaks observed for pure curcumin (*e.g.,* 1427, 1152, 961, 856, and 818 cm^{-1}) also disappeared when it was incorporated into saponin-coated nanoparticles, which is again indicative of a change in the environment and interactions of the curcumin molecules after encapsulation.

Information about the solid-state properties of the curcumin within the saponin-coated nanoparticles was obtained using X-ray diffraction. Diffraction peaks were detected for pure curcumin at 2θ values ranging from 5° to 30° (**Fig. 4)**, indicating that it was present in a highly crystalline structure [34]. Conversely, no diffraction peaks were observed for pure saponin, indicating that it was not in a crystalline state. Interestingly, no diffraction peaks were observed when the saponin-coated curcumin nanoparticles were analyzed, which suggests that the curcumin was in an amorphous form inside the particles. This result suggests that confinement of curcumin inside the saponin-coated nanoparticles inhibited its crystallization. This may be beneficial for certain delivery applications, since the bioavailability of amorphous forms of drugs has been shown to be higher than that of crystalline forms [35, 36].

3.3 Stability of curcumin nanoparticles

3.3.1. Impact of environmental stresses

The physical stability of colloidal delivery systems under different environmental conditions is important because it determines the range of commercial products that they can be successfully incorporated into, as well as their gastrointestinal fate [8]. For this reason, the influence of pH and ionic strength on the physicochemical properties of the curcumin nanoparticles was determined. Nanoparticle dispersions were adjusted to different pH values, then stored for 30 minutes, and then their appearance and mean particle diameter were measured. There was no visible change in the appearance of the colloidal dispersions after exposure to pH values ranging from 3 to 8, with all of them being transparent yellow/orange-colored fluids (**Fig. 5A**). Moreover, there was little change in the particle size in this pH range, with the mean particle diameter

459 remaining around 60 nm from pH 8 to 4, but increasing to around 81 nm at pH 3
460 (**Fig. 5A**). This result suggests that the saponin-coated curcumin nanoparticles
461 were relatively stable to aggregation in this pH range, which can be attributed to a
462 relatively strong electrostatic repulsion between them. Indeed, previous studies
463 on saponin-coated lipid nanoparticles have shown that they are highly negatively
464 charged at pH values of 4 and above, but lose their charge at lower pH values due
465 to protonation of the carboxyl groups [37].

466 The appearance of the colloidal dispersions became cloudy and the mean
467 particle diameter increased steeply when the pH was reduced to 2.0 and 1.5 **(Fig.**
468 **5A**). This effect can be attributed to extensive aggregation of the saponin-loaded
469 curcumin nanoparticles at pH values well below the pK_a values of the carboxyl
470 groups on the saponin (around pH 3.5), since this leads to a reduction in the
471 electrostatic repulsion between the nanoparticles [37, 38]. Indeed, electrophoresis
472 measurements indicated that the surface potential of the curcumin nanoparticles
473 was relatively low (-2.4 mV) at pH 2 in these systems. Other researchers have
474 also reported extensive aggregation of saponin-coated lipid nanoparticles at low
475 pH values [37], which was attributed to a similar mechanism.

476 The influence of ionic strength on the stability of the saponin-coated curcumin
477 nanoparticles was determined by incubating them in aqueous solutions containing
478 different NaCl levels (**Fig. 5B**). When the NaCl concentration was below 500
479 mM, the curcumin nanoparticles were relatively stable to aggregation without any
480 appreciable changes in their appearance or mean particle diameter. Visible
481 observation and particle size measurements indicated that they became unstable
482 to particle aggregation at 500 and 1000 mM NaCl. This phenomenon can be
483 attributed to the ability of cationic counter-ions (Na^+) in the salt solution to screen
484 the electrostatic repulsion between the saponin-coated nanoparticles [39]. As a
485 result, the net repulsive forces between the nanoparticles would not be strong
486 enough to overcome the net attractive forces (such as van der Waals), thereby
487 leading to aggregation [8].

3.3.2. Impact of long-term storage

The ability to remain stable during long-term storage is an important attribute of any colloidal delivery system that is going to have commercial viability. The physicochemical stability of the curcumin nanoparticles dispersed in aqueous solutions was therefore studied when they were stored at refrigerator (4 °C) or ambient temperature (25 °C) for one month (pH 6.5). In addition, the stability of freeze-dried curcumin nanoparticles was also measured after they were stored at 25 °C for one month and then rehydrated in aqueous solution (pH 6.5). There was little change in the appearance of the curcumin nanoparticle dispersions when stored at 4 °C in aqueous solutions or at 25 °C in powdered form (**Fig. 6A**). However, the appearance of the curcumin nanoparticle suspensions changed from yellow to brown, and there was visible evidence of particle aggregation, in the samples stored at 25 °C in the aqueous solutions. The change in appearance may have been due to chemical degradation and precipitation of curcumin, which is known to occur in aqueous solutions during long term storage at higher temperatures [40].

During storage, the mean diameter, ζ-potential, and encapsulation efficiency of the saponin-coated nanoparticles only changed slightly when they were stored at 4 °C in aqueous solutions or at 25 °C in powdered form (**Fig. 6B-D)**. Conversely, there was visible evidence of particle aggregation, a change in ζ-potential (from -29.8 to -11.0 mV), and a decrease in encapsulation efficiency (from 89.5 to 52.9%) when the curcumin nanoparticles were stored at 25 °C in aqueous solutions. Surprisingly, the mean diameter of the curcumin nanoparticles determined by dynamic light scattering exhibited little change during storage in the aqueous form at the higher temperature, even though flocculation was clearly visible by eye. This could be explained by the fact that the large slow-moving aggregates did not contribute to the DLS signal, which relies on particle motion to determine particle size. Overall, these results indicate that aqueous dispersions of curcumin nanoparticles were unstable if stored at

room temperature, but their stability could be improved by storing them at refrigeration temperatures or by converting them into a powder.

3.4 In Vitro Bioavailability of Curcumin

The *in vitro* bioavailability of curcumin in the saponin-coated nanoparticles was evaluated using a simulated gastrointestinal tract (GIT) and the results are expressed as the stability, bioaccessibility, and bioavailability (Section 2.5.2). The amount of curcumin in the small intestine remaining in the original form was appreciably higher for free curcumin (88.3%) than for encapsulated curcumin (54.0%) (**Fig. 7**), which suggests that curcumin degradation occurred more rapidly in saponin-coated nanoparticles than in free curcumin. In general, the degradation of curcumin in simulated GIT conditions primarily occurs due to its exposure to aqueous neutral or alkaline solutions [41]. The "free" curcumin used in our study consisted of relatively large curcumin crystals suspended in water, which would therefore be expected to have a lower specific surface area than curcumin encapsulated in nanoparticles. As a result, there would be less curcumin exposed to the surrounding aqueous phase for the free curcumin than for the encapsulated curcumin, leading to less chemical degradation. On the other hand, the bioaccessibility of free curcumin (9.1%) was appreciably lower than that of encapsulated curcumin (63.0%), which suggests that the nanoparticles greatly enhanced the solubility of curcumin in the dietary mixed micelles. This is probably because the curcumin nanoparticles had a much higher surface area and were in an amorphous form, and so they were dissolved and solubilized more rapidly than the larger curcumin crystals.

The *in vitro* bioavailability was taken to be equal to the total amount of curcumin solubilized in the mixed micelle phase, which takes into account both the bioaccessibility and transformation of the curcumin [41]. The bioavailability of curcumin in the nanoparticles (340.4 ± 13.4 μg/mL) was about 3.3-fold higher than for free curcumin (80.1 ± 2.1 μg/mL). This effect can be attributed to the much higher bioaccessibility of the curcumin in the nanoparticles than in the free

546 form. Overall, these results suggest that the *in vitro* bioavailability of curcumin
547 can be greatly increased by loading it into saponin-coated nanoparticles.

548 **3.5 *In Vivo* Bioavailability of Curcumin**

549 Experiments carried out using a simulated GIT cannot mimic the complexity
550 of an actual gastrointestinal tract, and so additional experiments were carried out
551 to determine the *in vivo* bioavailability using an animal model. Free curcumin and
552 curcumin nanoparticles were orally administered to rats at a dose of 100 mg/kg
553 body weight, and then the change in curcumin serum level over time was
554 measured (**Fig. 8**). A number of important pharmacokinetic parameters were then
555 calculated from these curves, including C_{max}, T_{max}, and $AUC_{0\text{-}8\ h}$ (**Fig. 8)**. After
556 oral administration of free curcumin, C_{max} was 0.47 μg/mL, T_{max} was 1 h, and
557 $AUC_{0\text{-}8\ h}$ was 1.43 μg h/mL. Curcumin was undetectable in the plasma after 4 h,
558 which indicated that it was rapidly removed. There was a significant ($P < 0.01$)
559 increase in C_{max} (6.91 μg/mL) and $AUC_{0\text{-}8\ h}$ (14.12 μg h/mL) and decrease in T_{max}
560 (0.5 h) after oral administration of the curcumin nanoparticles, when compared to
561 the free curcumin. The $AUC_{0\text{-}8\ h}$ value for the curcumin nanoparticles was
562 approximately 8.9-fold greater than that of free curcumin.

563 The appreciable increases in $AUC_{0\text{-}8\ h}$ and C_{max} values after encapsulation of
564 curcumin in saponin-coated nanoparticles indicated that they were highly
565 effective at enhancing curcumin bioavailability under *in vivo* conditions. This
566 effect may have been due to the ability of the nanoparticles to increase the
567 bioaccessibility and permeability of the curcumin in the animals GIT [42]. Indeed,
568 the shorter T_{max} value for the curcumin nanoparticles is indicative of a more rapid
569 absorption of curcumin across the epithelium layer. It is possible that saponin,
570 which is a natural surfactant, promoted the intestinal absorption of curcumin by
571 increasing the cell wall permeability, as had been reported for certain lipophilic
572 drugs [43]. In addition, a transcellular promoting effect may also have been caused
573 by interaction of the saponin with the membrane stabilizer cholesterol [44].
574 Nevertheless, more detailed studies are required to establish the precise origin of

the ability of the delivery systems to increase curcumin bioavailability.

In summary, both the *in vitro* and *in vivo* studies demonstrated that encapsulation of curcumin in saponin micelles greatly improved its bioavailability, which may be important for the development of more effective functional foods, supplements, or drugs.

4. Conclusions

This study has shown that curcumin nanoparticles can be formed from a natural surfactant (saponin) using a relatively rapid, simple, and inexpensive pH-driven method. These nanoparticles are relatively small (around 50 nm) and have a relatively high negative charge (around -30 mV). Moreover, their encapsulation efficiency (around 92%) and loading capacity (around 15%) are comparable or better than those achieved using synthetic surfactants. Encapsulation of curcumin within the nanoparticles greatly increased its *in vivo* bioavailability (8.9-fold compared to curcumin crystals), which was mainly attributed to their ability to increase the solubility of this hydrophobic nutraceutical within the small intestinal fluids.

This type of colloidal delivery system may therefore be useful for application in functional foods, supplements, or pharmaceutical preparations. Nevertheless, further work is required to determine the impact of incorporating these nanoparticles into specific food matrices on their quality attributes (such as appearance, texture, stability, and flavor profile). In addition, the potential toxicity of these nanoparticles should be established using acute and chronic testing methods. Finally, the potential efficacy of these curcumin nanoparticles at improving health outcomes should be established.

Acknowledgements

We appreciate the financial support by the National Science Foundation of China (No. 21766018, 31601468), Technical Leader Training Plan Project of Jiangxi Province (20162BCB22009) and the Key Project of Natural Science

Foundation of Jiangxi Province, China (20171ACB20005). This material is partly based upon work supported by the National Institute of Food and Agriculture, USDA, Massachusetts Agricultural Experiment Station (MAS00491) and USDA, AFRI Grants (2014-67021, 2016-25147, and 2016-08782).

References

1. P. Anand, A. B. Kunnumakkara, R. A. Newman and B. B. Aggarwal, *Molecular pharmaceutics*, 2007, **4**, 807-818.
2. M. Heger, R. F. van Golen, M. Broekgaarden and M. C. Michel, *Pharmacological reviews*, 2014, **66**, 222-307.
3. G. Zhou, Y. Peng, L. Zhao, M. Wang and X. Li, *Journal of agricultural and food chemistry*, 2017, **65**, 1518-1524.
4. F. Bai, J. Diao, Y. Wang, S. Sun, H. Zhang, Y. Liu, Y. Wang and J. Cao, *Journal of agricultural and food chemistry*, 2017, **65**, 6840-6847.
5. J. Xiao, Y. Cao and Q. Huang, *Journal of agricultural and food chemistry*, 2017, **65**, 6727-6735.
6. L. K. Mao and S. Miao, *Food Engineering Reviews*, 2015, **7**, 439-451.
7. P. A. Darne, M. R. Mehta, S. B. Agawane and A. A. Prabhune, *RSC Advances*, 2016, **6**, 68504-68514.
8. D. J. McClements, *Food Emulsions: Principles, Practices, and Techniques*, CRC Press, Boca Raton, FL, 3rd edn., 2015.
9. J. Tippel, M. Lehmann, R. von Klitzing and S. Drusch, *Food Chemistry*, 2016, **212**, 35-42.
10. D. J. McClements and C. E. Gumus, *Advances in Colloid and Interface Science*, 2016, **234**, 3-26.
11. S. Bottcher and S. Drusch, *Advances in Colloid and Interface Science*, 2017, **243**, 105-113.
12. H. Barakat, V. Reim and S. Rohn, *Food Research International*, 2015, **76**, 142-149.
13. K. R. Price, I. T. Johnson and G. R. Fenwick, *Critical reviews in food science and nutrition*, 1987, **26**, 27-135.
14. B. Singh, J. P. Singh, N. Singh and A. Kaur, *Food Chemistry*, 2017, **233**, 540-549.
15. J. Shi, S. J. Xue, Y. Ma, D. Li, Y. Kakuda and Y. Lan, *Journal of Food Engineering*, 2009, **93**, 59-65.
16. X. Luo, Y. Zhou, L. Bai, F. Liu, R. Zhang, Z. Zhang, B. Zheng, Y. Deng and D. J. McClements, *Food Research International*, 2017, **96**, 103-112.
17. C. Chung, A. Sher, P. Rousset and D. J. McClements, *Food Research International*, 2017, DOI: 10.1016/j.foodres.2017.06.060.
18. C. Cheng, S. Peng, Z. Li, L. Zou, W. Liu and C. Liu, *RSC Advances*, 2017, **7**, 25978-25986.
19. Y. Mao and D. J. McClements, *Food & function*, 2012, **3**, 1025-1034.
20. D. J. McClements, F. Li and H. Xiao, in *Annual Review of Food Science and Technology, Vol 6*, eds. M. P. Doyle and T. R. Klaenhammer, 2015, vol. 6, pp. 299-327.
21. M. Shoji, K. Nakagawa, A. Watanabe, T. Tsuduki, T. Yamada, S. Kuwahara, F. Kimura and T. Miyazawa, *Food Chemistry*, 2014, **151**, 126-132.
22. K. Nakagawa, T. Harigae, T. Miyazawa, N. Inoue, F. Kimura, I. Ikeda and T. Miyazawa, *International Journal of Nanomedicine*, 2016, **Volume 11**, 3009-3022.
23. R. Vecchione, V. Quagliariello, D. Calabria, V. Calcagno, E. De Luca, R. V. Iaffaioli and P. A. Netti, *Journal of controlled release : official journal of the Controlled Release Society*, 2016, **233**, 88-

100.
24. K. Pan, Y. C. Luo, Y. D. Gan, S. J. Baek and Q. X. Zhong, *Soft Matter*, 2014, **10**, 6820-6830.
25. S. Mitra and S. R. Dungan, *Journal of agricultural and food chemistry*, 1997, **45**, 1587-1595.
26. J. Tippel, K. Gies, B. Harbaum-Piayda, A. Steffen-Heins and S. Drusch, *Food Chemistry*, 2017, **221**, 386-394.
27. R. Ganguly, A. Kunwar, B. Dutta, S. Kumar, K. C. Barick, A. Ballal, V. K. Aswal and P. A. Hassan, *Colloids and surfaces. B, Biointerfaces*, 2017, **152**, 176-182.
28. H. Kheiri Manjili, P. Ghasemi, H. Malvandi, M. S. Mousavi, E. Attari and H. Danafar, *European journal of pharmaceutics and biopharmaceutics : official journal of Arbeitsgemeinschaft fur Pharmazeutische Verfahrenstechnik e.V*, 2017, **116**, 17-30.
29. P. R. K. Mohan, G. Sreelakshmi, C. V. Muraleedharan and R. Joseph, *Vibrational Spectroscopy*, 2012, **62**, 77-84.
30. M. S. Almutairi and M. Ali, *Natural product research*, 2015, **29**, 1271-1275.
31. G. Mandal and A. K. Nandi, *International Journal of Pharmacy and Pharmaceutical Sciences*, 2013, **5**, 517-523.
32. C. Sun, C. Xu, L. Mao, D. Wang, J. Yang and Y. Gao, *Food Chemistry*, 2017, **228**, 656-667.
33. X. Chen, L. Q. Zou, J. Niu, W. Liu, S. F. Peng and C. M. Liu, *Molecules*, 2015, **20**, 14293-14311.
34. J. Li, G. H. Shin, I. W. Lee, X. Chen and H. J. Park, *Food Hydrocolloids*, 2016, **56**, 41-49.
35. R. Jog and D. J. Burgess, *Journal of Pharmaceutical Sciences*, 2017, **106**, 39-65.
36. P. Kanaujia, P. Poovizhi, W. K. Ng and R. B. H. Tan, *Powder Technology*, 2015, **285**, 2-15.
37. B. Ozturk, S. Argin, M. Ozilgen and D. J. McClements, *Journal of Food Engineering*, 2014, **142**, 57-63.
38. Y. Yang, M. E. Leser, A. A. Sher and D. J. McClements, *Food Hydrocolloids*, 2013, **30**, 589-596.
39. W. Liu, W. Liu, A. Ye, S. Peng, F. Wei, C. Liu and J. Han, *Food Chemistry*, 2016, **196**, 396-404.
40. M. Kharat, Z. Y. Du, G. D. Zhang and D. J. McClements, *Journal of agricultural and food chemistry*, 2017, **65**, 1525-1532.
41. L. Zou, B. Zheng, R. Zhang, Z. Zhang, W. Liu, C. Liu, H. Xiao and D. J. McClements, *RSC Advances*, 2016, **6**, 3126-3136.
42. M. Anwar, I. Ahmad, M. H. Warsi, S. Mohapatra, N. Ahmad, S. Akhter, A. Ali and F. J. Ahmad, *European journal of pharmaceutics and biopharmaceutics : official journal of Arbeitsgemeinschaft fur Pharmazeutische Verfahrenstechnik e.V*, 2015, **96**, 162-172.
43. E. Moghimipour, S. A. S. Tabassi, M. Ramezani, S. Handali and R. Lobenberg, *Journal of Advanced Pharmaceutical Technology & Research*, 2016, **7**, 75-79.
44. Shaikh, *Journal of Applied Pharmaceutical Science*, 2012, DOI: 10.7324/japs.2012.2705.

679 # Tables

680 **Table 1.** Physicochemical characteristics and structural properties of (A) fresh
681 prepared curcumin-loaded micelles and (B) redispersed lyophilized curcumin-
682 loaded micelles with different saponin concentrations (pH 6.5). The curcumin
683 concentration was 1 mg/mL in all samples.

	Saponin concentration (mg/mL)	Mean diameter (nm)	Polydispersity index	ζ-potential (mV)	Encapsulation efficiency (%)
A	1	108.6 ± 13.9 [b]	0.191 ± 0.011 [a]	-31.92 ± 0.45 [a]	71.2 ± 2.7 [b]
	2	87.9 ± 7.0 [b]	0.275 ± 0.057 [a]	-30.31 ± 0.55 [a]	87.9 ± 1.9 [c]
	4	**51.9 ± 3.0** [a]	**0.242 ± 0.045** [a]	**-30.44 ± 0.43** [a]	**91.8 ± 2.8** [c]
	6	48.8 ± 0.9 [a]	0.168 ± 0.027 [a]	-25.36 ± 1.59 [b]	92.9 ± 1.6 [c]
	8	49.7 ± 2.7 [a]	0.163 ± 0.028 [a]	-19.18 ± 1.63 [d]	93.2 ± 3.9 [c]
B	1	223.5 ± 38.3 [c]	0.609 ± 0.098 [c]	-29.83 ± 0.57 [a]	44.1 ± 7.1 [a]
	2	115.6 ± 1.6 [b]	0.417 ± 0.025 [b]	-31.22 ± 0.73 [a]	72.8 ± 1.0 [b]
	4	**50.3 ± 0.4** [a]	**0.217 ± 0.009** [a]	**-29.56 ± 0.57** [a]	**87.1 ± 2.4** [c]
	6	49.5 ± 0.8 [a]	0.164 ± 0.024 [a]	-21.35 ± 0.96 [c]	89.8 ± 0.6 [c]
	8	50.8 ± 0.5 [a]	0.203 ± 0.020 [a]	-17.40 ± 1.34 [d]	91.2 ± 0.4 [c]

684

685 **Figure captions**

686 **Fig. 1** Schematic representation of the formation of curcumin nanoparticles using the
687 pH-driven loading mechanism: (A) the chemical structure and symbol of curcumin and
688 saponin, (B) an acidic saponin micelle solution is mixed with a basic curcumin solution,
689 which promotes curcumin molecules to move into the hydrophobic micelle core, (C) the
690 pH change with time when the saponin was mixed with the curcumin.

691 **Fig. 2** Atomic forces microscopy image of curcumin nanoparticles formed using the pH-
692 driven loading mechanism.

693 **Fig. 3** FTIR spectrum of (a) curcumin, (b) saponin and (c) saponin-coated curcumin
694 nanoparticles.

695 **Fig. 4** XRD spectra of curcumin, saponin and saponin-coated curcumin nanoparticles.

696 **Fig. 5** Effect of (A) pH values and (B) NaCl concentration on the particle size and
697 appearance of saponin-coated curcumin nanoparticles.

698 **Fig. 6** Physicochemical stability of saponin-coated curcumin nanoparticles stored in
699 liquid aqueous suspensions at 4 and 25 °C, or powders at 25 °C for one month: (A)
700 change of appearance, (B) change of encapsulation efficiency, (C) change of average
701 diameter, (D) change of ζ-potential.

702 **Fig. 7** The stability and bioaccessibility of free curcumin and saponin-coated curcumin
703 nanoparticles after passing through a simulated gastrointestinal tract.

704 **Fig. 8** *In vivo* bioavailability of curcumin delivered in free form or as saponin-coated
705 nanoparticles. (Inset) Pharmacokinetics parameters of the different curcumin samples.
706 Key: AUC = area under the plasma concentration−time curve from 0 to 8 h; C_{max} = peak

707 concentration; T_{max} = time to reach peak concentration.

708 Fig. 1

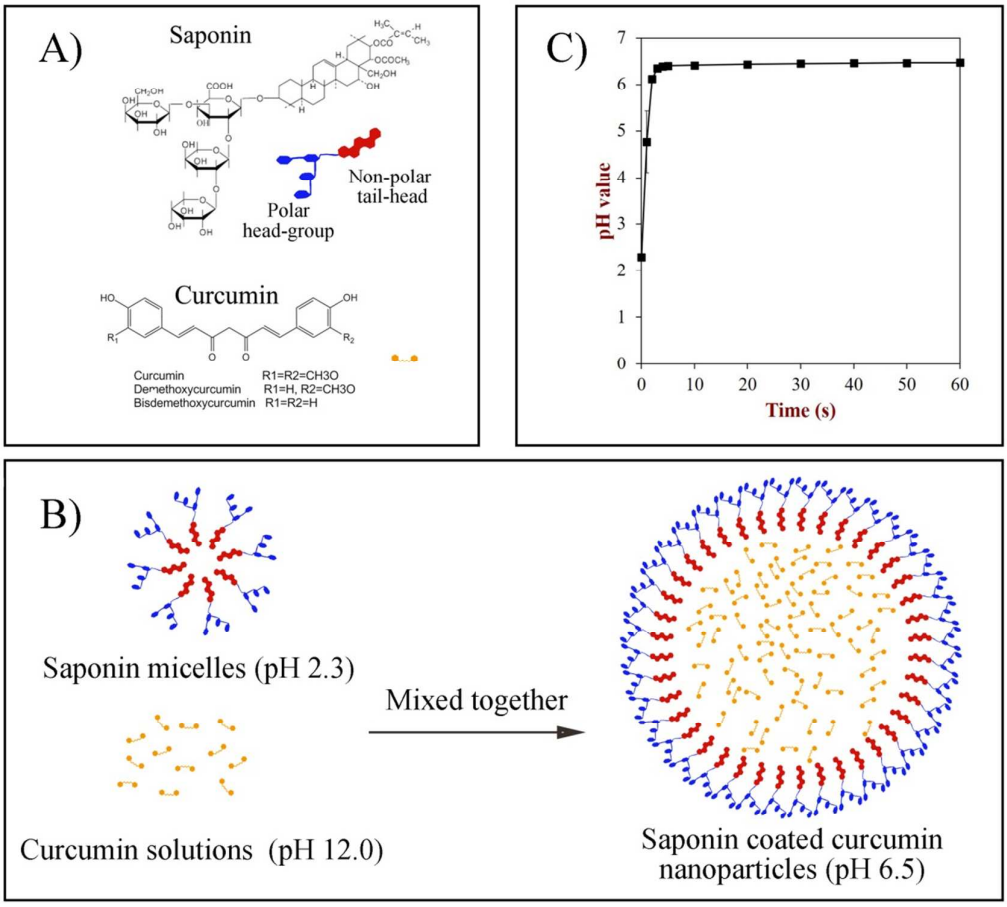

709

710

711 **Fig. 2**

712

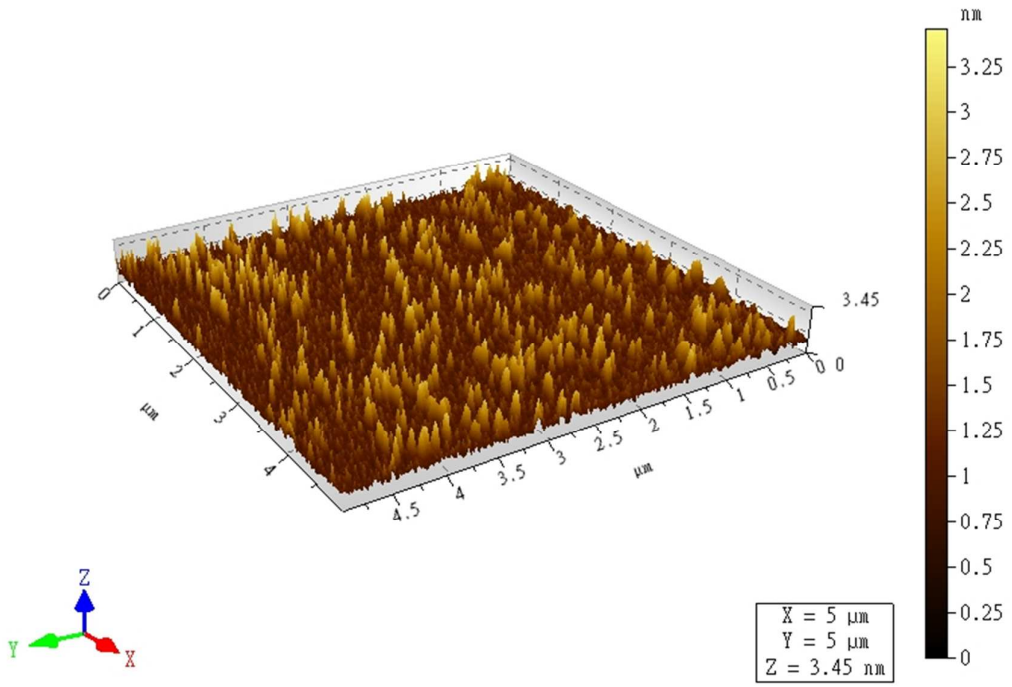

713

714

715 **Fig. 3**

716

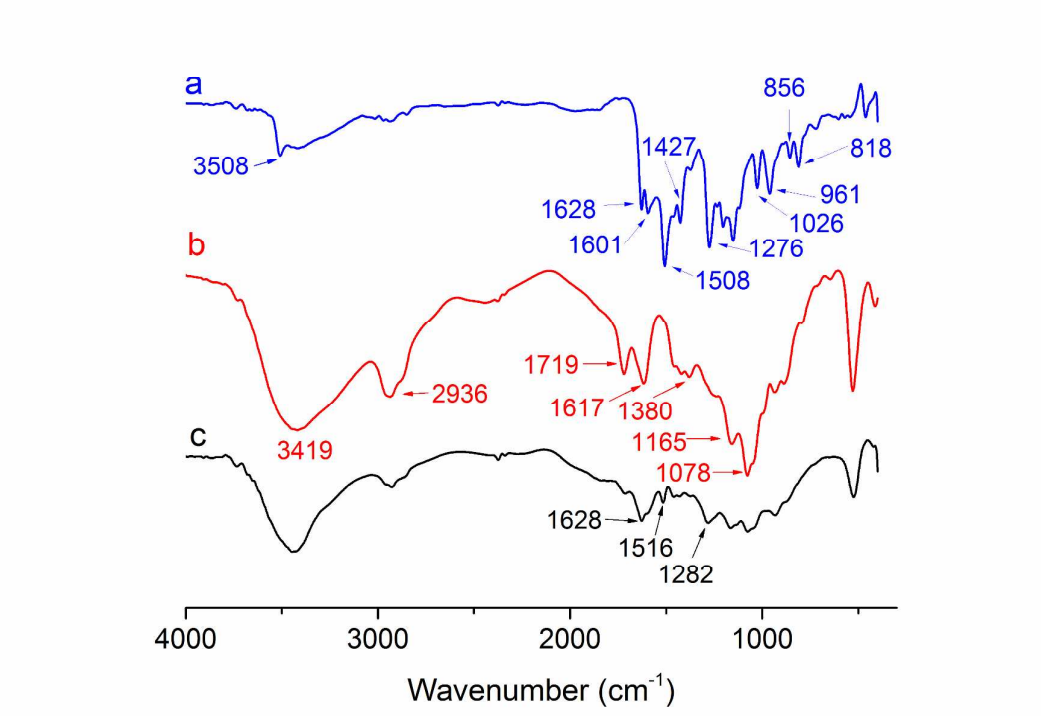

717

718 **Fig. 4**

719

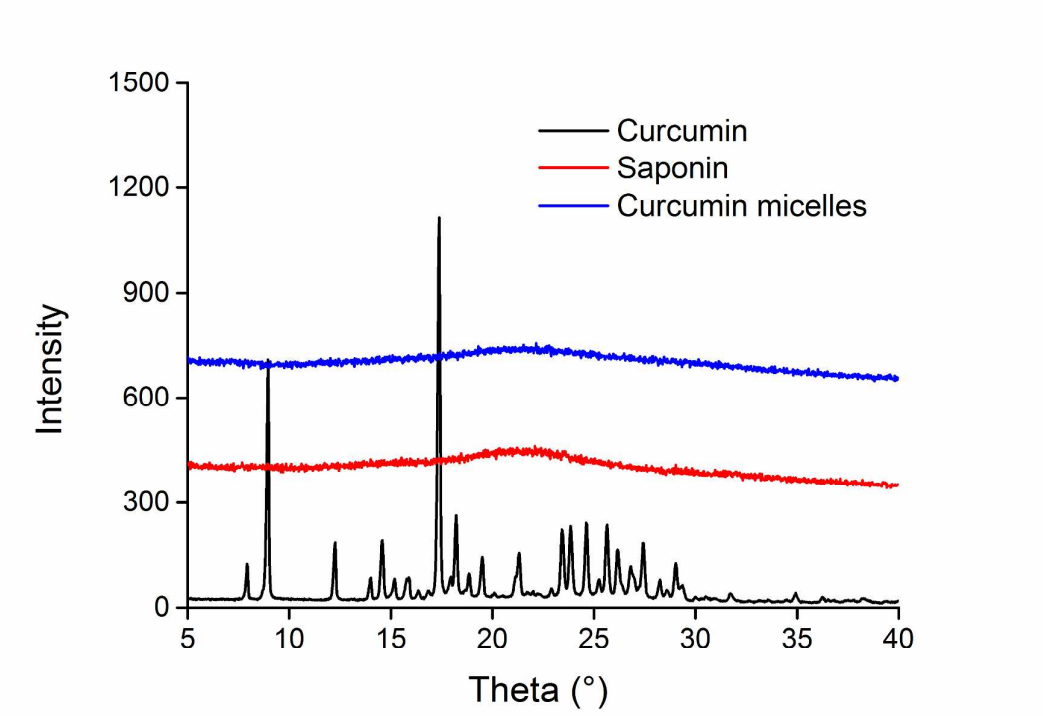

720

721

722 **Fig. 5**

723

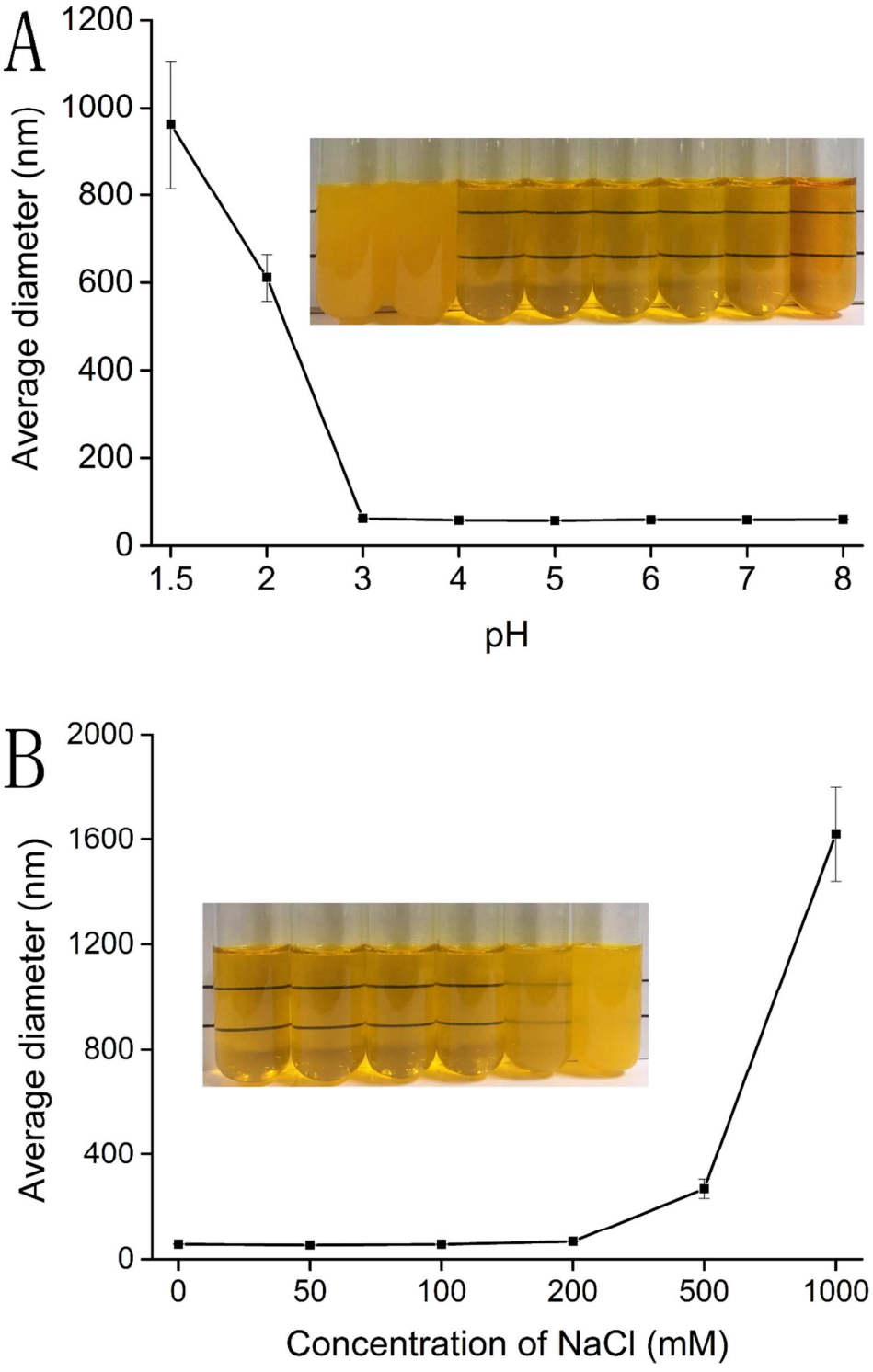

724

725 **Fig. 6**

726

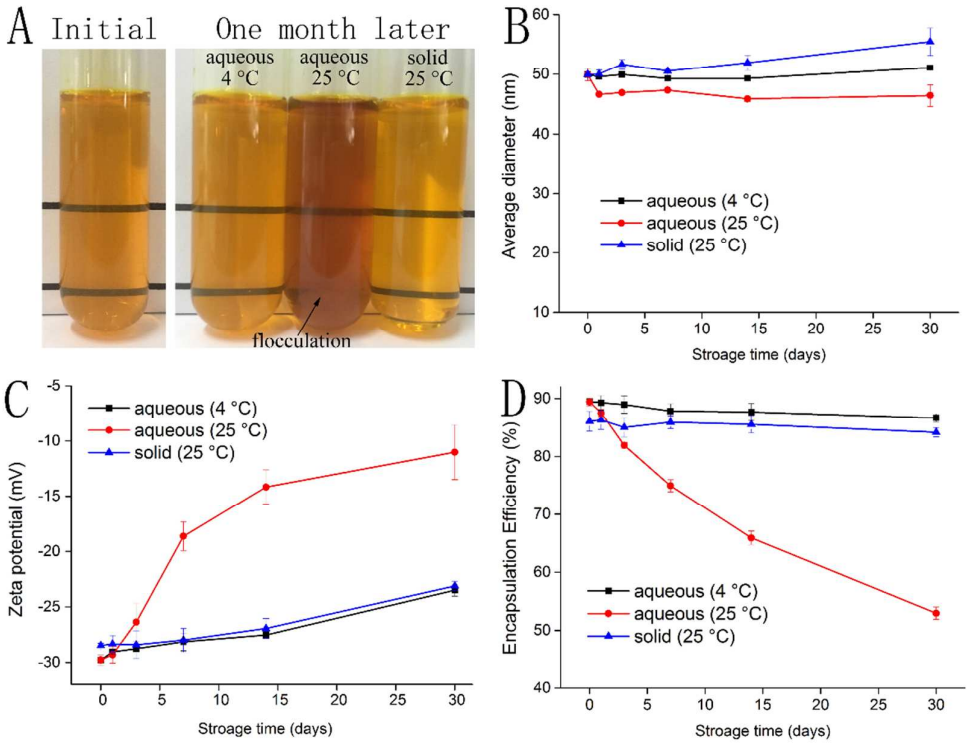

727

728

729 **Fig. 7**

730

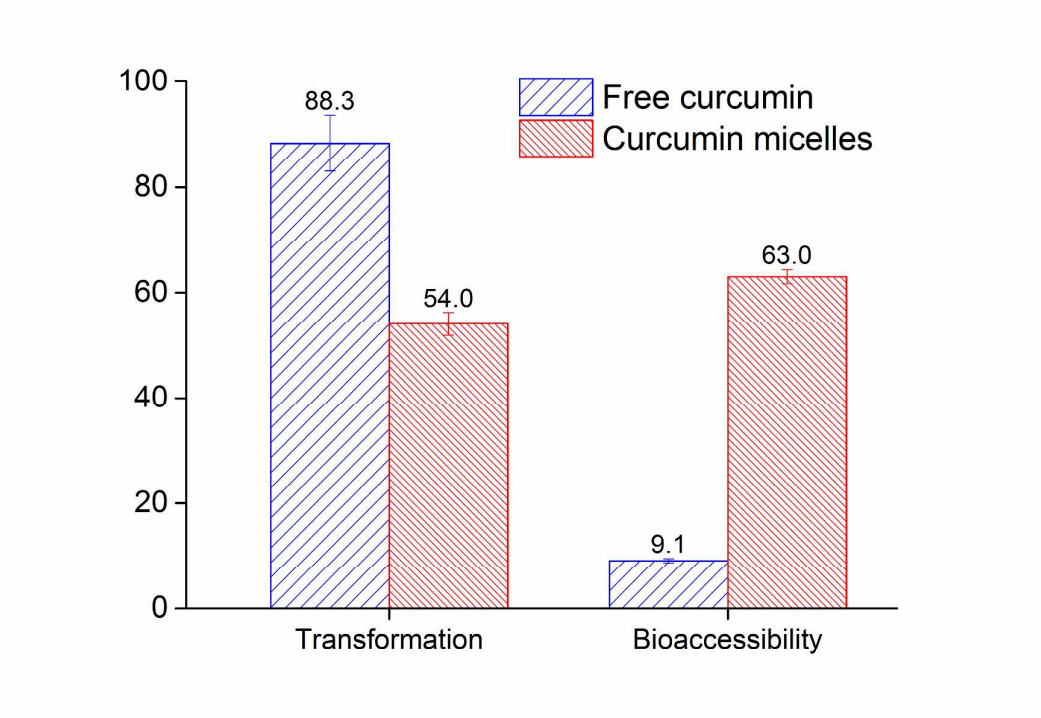

731

732

733 **Fig. 8**

734

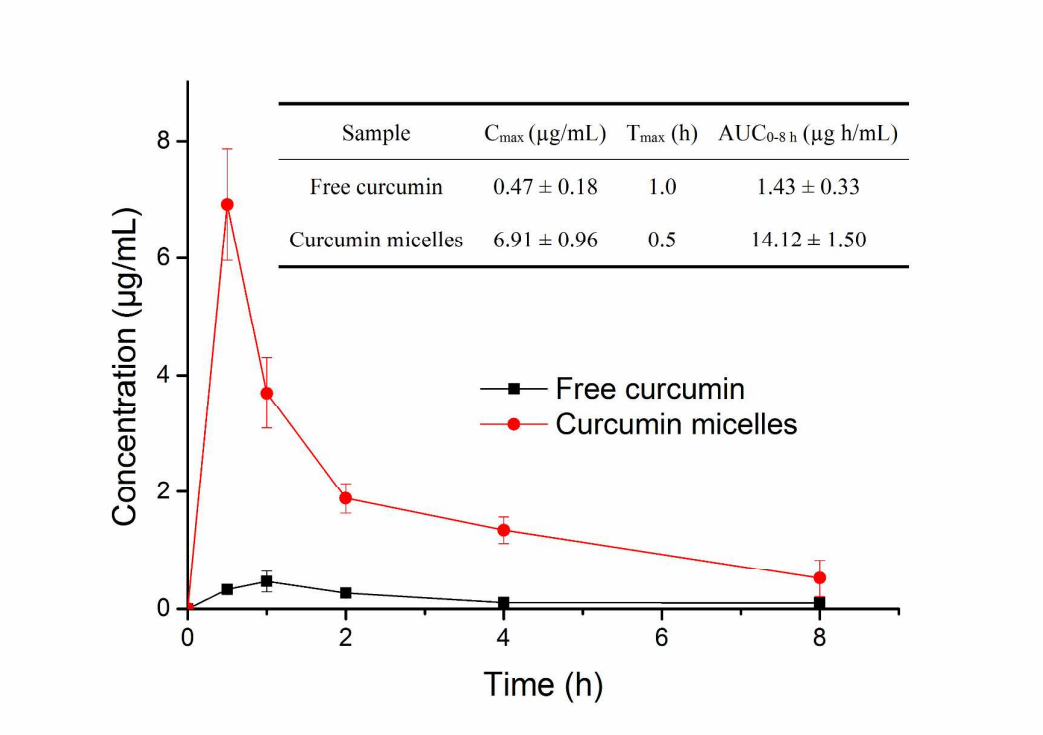

735

736

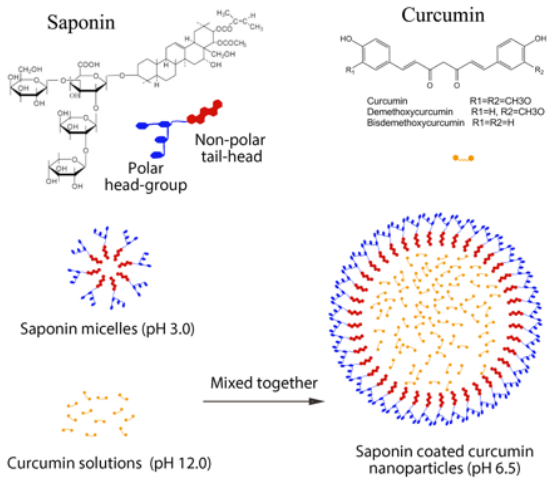
Saponin
Curcumin
Curcumin R1=R2=CH3O
Demethoxycurcumin R1=H, R2=CH3O
Bisdemethoxycurcumin R1=R2=H
Non-polar tail-head
Polar head-group
Saponin micelles (pH 3.0)
Mixed together
Curcumin solutions (pH 12.0)
Saponin coated curcumin nanoparticles (pH 6.5)